Polyketone Polymers Prepared Using a Palladium/Alumoxane Catalyst System

Yoshihiro Koide and Andrew R. Barron*

Department of Chemistry, Rice University, Houston, Texas 77005, and Department of Chemistry, Harvard University, Cambridge, Massachusetts 02138

Received September 12, 1995; Revised Manuscript Received November 7, 1995®

ABSTRACT: The palladium-catalyzed copolymerization of carbon monoxide and ethylene to give polyketone polymers, $[-CH_2CH_2C(O)-]_n$, has been accomplished by the use of either $(dppp)Pd(OAc)_2$ or $(dppp)Pd[C(O)^tBu]Cl$ in the presence of the *tert*-butyl alumoxane $[(^tBu)AlO]_6$ as a cocatalyst. The polymers were characterized by X-ray diffraction (XRD), scanning electron microscopy (SEM), IR and multinuclear NMR spectroscopy, thermogravimetric/differential thermal analysis (TG/DTA), gas desorption, solution molecular weight, and intrinsic viscosity. All the polymers ($16\,700 < M_n < 58\,400$) were shown to be perfectly alternating $CO/H_2C{=}CH_2$ and crystalline (α-phase). The crystallographic density of the polymers was found to be high ($1.445\ g{\cdot}cm^{-3}$). Crystallinity is retained upon recrystallization and melting, although transition to the β-phase occurs after heating at 160 °C for 100 h. The dependence of polymer yield and molecular weight on reaction temperature and pressure was determined. Thin films of polyketone polymer have been formed from $HOC(H)(CF_3)_2$ solution. Terpolymers, $[C(H)(R)CH_2C(O)]_m[CH_2CH_2C(O)]_n$, are prepared using 1-octene or 4-phenyl-1-butene in addition to ethylene and CO. The maximum level of incorporation of a second olefin is $m{:}n = 1{:}24$ and is presumably related to the increased steric hindrance of the substituted olefin. No polymerization is observed for CO and either 1-octene or 4-phenyl-1-butene in the absence of ethylene. The properties of the polyketone polymers are compared to those prepared by other routes, in particular the higher density and increased phase stability.

Introduction

The copolymerization of ethylene and carbon monoxide to give polyketones, eq 1, has been known since the seminal work on peroxide-initiated radical copolymer-

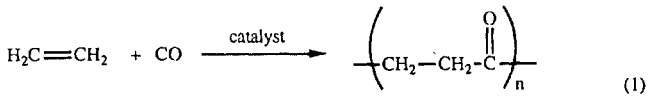

(I) (1)

ization by Brubaker and co-workers.[1] While many commercial polyethylene-based polymers contain a few carbonyl groups (e.g., <1 wt % in beer "six-pack" yokes), truly alternating polyketones (**I**) show higher mechanical strengths than polyolefins.[2] It is as a consequence of their potential commercial significance, that there has been much interest in the development of new synthetic routes to polyketones.[3]

Initial routes involved radical copolymerization at high pressures, while, more recently, transition metal-catalyzed systems under moderate pressures have been developed. While the original transition metal catalyst systems employed either Ni(II)[4] and Pd(II)[5] cyanides or neutral tertiary phosphine complexes of Pd(II) or Pt(0),[6] subsequent work by Sen and co-workers[7,8] showed that the preformed cationic palladium complexes $[Pd(PPh_3)_n(MeCN)_{4-n}][BF_4]$ were capable of copolymerizing olefins with carbon monoxide under mild conditions. As was demonstrated by workers at Shell, a significant increase in activity is observed by the use of chelating phosphines and the in-situ formation of the cationic palladium catalyst from the reaction of $[R_2P(CH_2)_3PR_2]$-$Pd(OAc)_2$ (e.g., R = *o*-$MeOC_6H_4$) with noncoordinating acids (e.g., HBF_4).[9] In recent years there has been a plethora of catalyst systems reported;[10−14] however, all the systems are based upon a cationic transition metal center, $[L_nMX]^+$, and a noncoordinating anion.

The cationic zirconocene, $[Cp_2Zr(R)]^+$, polymerization of ethylene has been extensively investigated,[15] and while a number of "noncoordinating" anions have been reported[16] the most commonly employed is methylalumoxane (MAO).[17] Recent work in the patent literature indicates that alumoxanes could also be used as cocatalysts in polyketone synthesis.[18] We have recently reported the first isolation and structural characterization of alumoxanes.[19,20] Furthermore, we have shown that alumoxanes have cage structures, $[(^tBu)AlO]_n$ (n = 6, 7, 8, 9, 12), which are electron precise, and their catalytic activity is related to their "Latent Lewis acidity".[21] Our ability to isolate individual alumoxanes has prompted us to study the palladium−alumoxane-catalyzed copolymerization of ethylene and carbon monoxide. The results of this study are presented herein.

Results and Discussion

The ethylene/carbon monoxide copolymerizations were carried out by a modification of our previously reported procedures. As a general procedure, a CH_2Cl_2 solution of $[(^tBu)AlO]_6$ (**II**) was added to a solution of either $(dppp)Pd(OAc)_2$ (**III**) or $(dppp)Pd[C(O)^tBu]Cl$ (**IV**) previously purged with CO in a Teflon-lined autoclave (see Experimental Section).

The reaction mixture was then pressurized to 100−400 psi[22] with a premixed equimolar mixture of CO and ethylene, and heated to 30−120 °C. The pressure of the vessel was monitored during the course of the reaction. The reaction was quenched by release of the CO/ethylene pressure upon completion of the polymerization. The polymer was isolated by filtration and washing. A summary of the polymerization reaction conditions is given in Table 1.

In order to test the resilience of the catalyst with respect to continued polymerization, a reaction was performed in which the autoclave was continually

* Address all correspondence to this author at Department of Chemistry, Rice University, 6100 Main St. Houston, TX 77005.
® Abstract published in *Advance ACS Abstracts,* January 15, 1996.

0024-9297/96/2229-1110$12.00/0

Table 1. Summary of Catalysis Conditions and Polyketone Characterization

sample	temp (°C)	pressure (psi)[a]	yield (mg)[b]	T_m (°C)	mass loss (%)[c]	M_w[d]	M_n[d]	R	inherent viscocity ($cm \cdot g^{-1}$)[d,e]	surface area ($m^2 \cdot g^{-1}$)
1	30	300	50	237.6	6.5	81 600	20 100	4.06	3.012 (1.53)	21
2	60	100	61	229.1	6.4	62 900	16 700	3.77		72
3	60	200	133	238.6	7.2	108 000	30 000	2.99	2.219 (1.78)	78
4	60	300	232	246.0	1.7	122 000	57 100	2.13	(2.34)	53
5	60	400	416	251.4	1.8	120 000	58 400	2.05	(3.18)	<0.2
6	75	300	395	235.9	11.9	111 000	20 200	5.51	2.453 (2.33)	18
7	90	300	189	224.8	2.4	87 700	21 500	4.09	2.744	34
8	120	300	111	215.2	5.8	56 500	6 150[f]	9.18[f]		42

[a] Initial pressure of ethylene/CO (50:50). [b] Isolated yield. [c] Mass loss upon melting. [d] Measured in $HOC(H)(CF_3)_2$. [e] Values in parentheses measured in *p*-cresole. [f] Sample contained significant low molecular weight material.

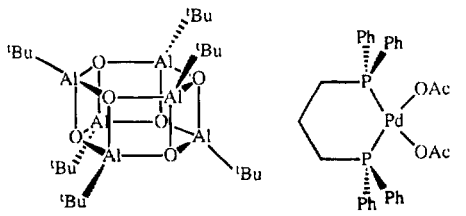

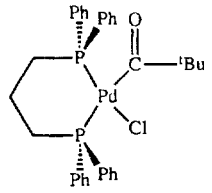

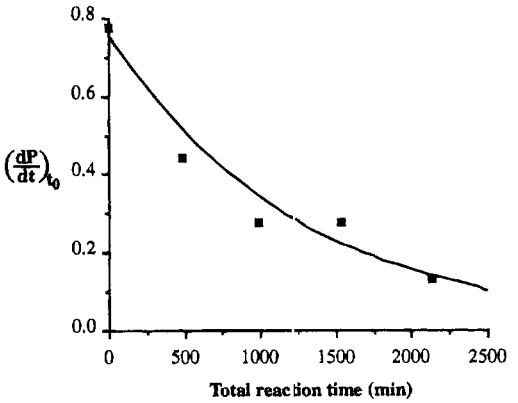

Figure 1. Plot of polymerization rate (dP/dt) versus total reaction time (min) of catalysis, using (dppp)$Pd(OAc)_2$ (0.36 mM) and TBAO (*ca.* 33 mM "Al") in CH_2Cl_2.

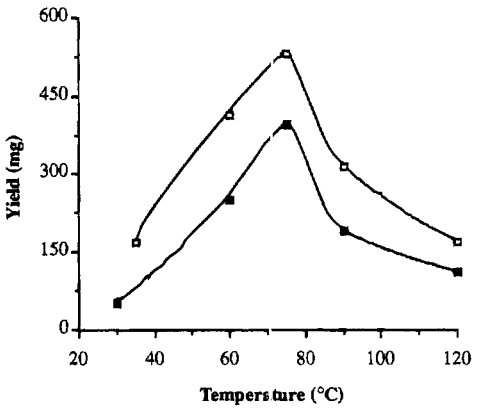

Figure 2. Polyketone yield (mg) as a function of reaction temperature (°C). Reactions were performed over 2 h, under 300 psi, in CH_2Cl_2, with (dppp)$Pd(OAc)_2$ (■) or (dppp)Pd[C(O)^{t}Bu]Cl (□) (0.33 mM) and $[(^tBu)AlO]_6$ (1.67 mM).

repressurized to the initial pressure, and the initial rate was determined. In Figure 1 is shown a plot of initial rate (dP/dt) at t_0 versus total time of catalyst activity for a series of pressurization/polymerization cycles. It can be clearly seen that the rate of polymerization slowly decreases until the catalyst essentially loses activity at 44 h. Since no evidence is seen for the formation of Pd(0), as a consequence of catalyst decomposition, the decrease in catalyst activity with time is either due to the formation of a stable Pd(II) compound or diffusion inhibition of reactants to the palladium center.

Temperature, Pressure, and Solvent Effects on Catalysis. As is seen in Figure 2, the yield of polymer using both (dppp)$Pd(OAc)_2$ and (dppp)Pd[C(O)^{t}Bu]Cl increases with increased reaction temperature up until *ca.* 75 °C, at which point the polymer yield decreases. The shape of the curves is consistent with an increase of inherent polymerization rate with increased temperature and a decrease of catalyst lifetime with increased temperature. Thus, below 75 °C the catalyst is slow but still active after the 2 h reaction time. Above 75 °C the catalyst is "dead" before the reaction time is complete.[23]

Under the conditions employed, the rate of polymerization varies linearly with both the total gas pressure (Figure 3) and the partial pressures of the individual reagents (Figure 4). The observation that the rate of polymerization is essentially linear with respect to each gas suggests that under the conditions employed saturation kinetics do not apply; i.e., the reaction is mass transport limited.

As with any catalytic system the solvent has an effect on the rate of copolymerization of carbon monoxide and ethylene. While the optimum solvent was found to be CH_2Cl_2, several other nonprotic solvents were investigated. As can be seen from Figure 5, nonpolar solvents gave low yields, as did coordinating solvents. The low polymer yield for reactions in THF and MeCN is most likely due to the competitive complexation of the Lewis acidic solvent to palladium in place of CO or $H_2C{=}CH_2$. The low yield in nonpolar hydrocarbon solvents is undoubtedly related to the observed low solubility of the palladium catalyst therein.

Characterization of the Ethylene–Carbon Monoxide Polyketone Polymer. A summary of selected polyketone characterization is given in Table 1. All the polyketone polymers isolated are white in color with a fluffy appearance, as seen in Figure 6. It is worth noting that increased reaction pressure results in a fluffier appearance of the polymer. In Figure 7a is shown a scanning electron micrograph of a representative sample of polyketone prepared at 60 °C and 300 psi initial pressure, using (dppp)$Pd(OAc)_2$ and $[(^tBu)AlO]_6$ as the cocatalyst. The alumoxane-catalyzed polymer consists of spherical particles between 5 and 20 μm

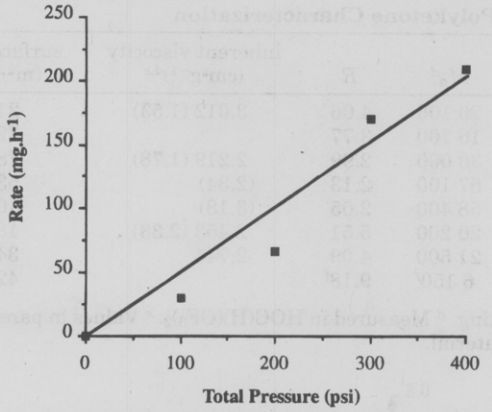

Figure 3. Polymerization rate ($mg \cdot h^{-1}$) as a function of initial (total) pressure (psi). Reactions were performed over 2 h, at 60 °C, with (dppp)$Pd(OAc)_2$ (0.33 mM) and $[(^tBu)AlO]_6$ (1.67 mM) in CH_2Cl_2.

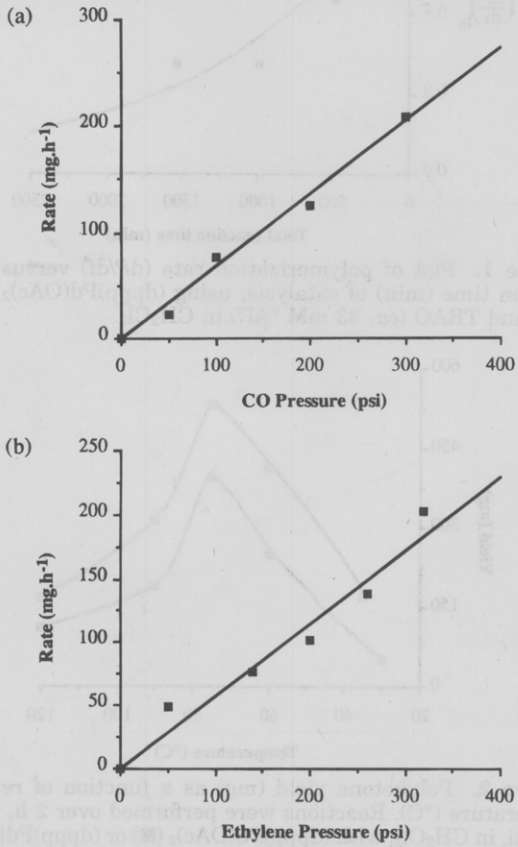

Figure 4. Polymerization rate ($mg \cdot h^{-1}$) as a function of initial CO (a) and ethylene (b) partial pressure (psi). Reactions were performed over 2 h, at 60 °C, with (dppp)$Pd(OAc)_2$ (0.33 mM) and $[(^tBu)AlO]_6$ (1.67 mM) in CH_2Cl_2. In each case a base pressure of 100 psi was used for the invariant gas.

in diameter. As can be seen from Figure 7b, each particle is highly porous spongelike. The morphology of the polymers is systemic of the even growth of the polymer throughout polymerization. The porous nature of the polymers is confirmed by gas desorbtion surface area measurements (Table 1). The surface area of all the polymers is in the range 18–80 $m^2 \cdot g^{-1}$. While there is no definitive trend between surface area and the reaction temperature, polymers produced at higher initial pressures generally have lower surface areas.

Despite the porous nature of the as prepared polymer, contiguous uniform films may be formed from the evaporation of $HOC(H)(CF_3)_2$ solutions. As is seen from the SE image in Figure 8, the films, while uniform, have

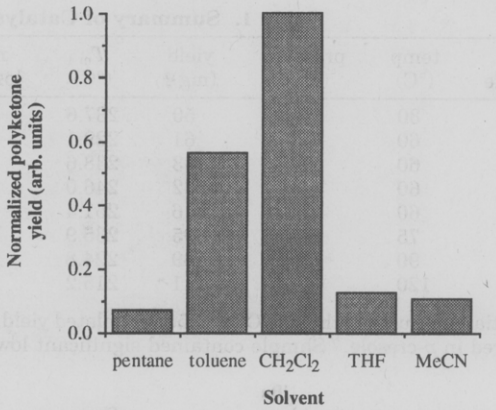

Figure 5. Normalized polyketone yield (arbitrary units) as a function of solvent. Reactions were performed over 2 h, at 60 °C, with (dppp)$Pd(OAc)_2$/$[(^tBu)AlO]_6$ under and 300 psi initial pressure (CO, $H_2C{=}CH_2$).

Figure 6. Polyketone samples prepared with initial reaction pressures of 200, 300 and 400 psi. Note, the fluffy appearance of the polymer prepared at the higher pressure.

some macroscopic pores due to the rapid evaporation of the solvent; however, the surface may be controlled in part by the solution concentration.

Spectroscopically, the polyketone polymers prepared using alumoxane cocatalysts are identical to those previously reported.[24] The IR spectra show a sharp band at 1692 cm^{-1} due to the $\nu(C{=}O)$ stretch, and a band at 1259 cm^{-1} due to the $\nu(C{=}C)$ stretch. The CPMAS ^{13}C NMR spectra (Figure 9a) show two single resonances due to the carbonyl (δ 212) and alkene (δ 38.5) carbons, while the solution ^{13}C NMR spectra (Figure 9b) show similar resonances (δ 212, 35.6). The ^1H NMR spectra consist of essentially a single resonance (δ 2.43). It should be noted that no additional peaks systemic of the polymer termini are observed in either ^1H or ^{13}C NMR spectra, suggestive of M_n being greater than 20 000. It is also worth noting that no peaks are observed that can be assigned as being due to either cross-linking or furanization.[25]

All the polymers are soluble in $HOC(H)(CF_3)_2$, allowing for the measurement of solution molecular weights (M_w and M_n). Data for the polyketones are presented in Table 1 and confirm the high molecular weights (M_n = 16 700–58 400, M_w = 56 500–122 000[26]) of the polymers. Furthermore, the inherent viscocities (see Table 1) are comparable to the values previously reported.[12] It is interesting to note that the polydispersity, R, decreases with increasing M_w and M_n. The relationship of the polyketone solution molecular weight as a function of reaction temperature is shown in Figure 10. The molecular weight of the polyketone polymers reaches a maximum between 50 and 60 °C, above which the molecular weight decreases. Given that a similar curve is observed for the temperature dependence of the polymer yield (see Figure 2), it is tempting to assume that the same factors apply, i.e., that catalyst decomposition at higher temperatures results in the formation of a low yield of low molecular weight polymers.

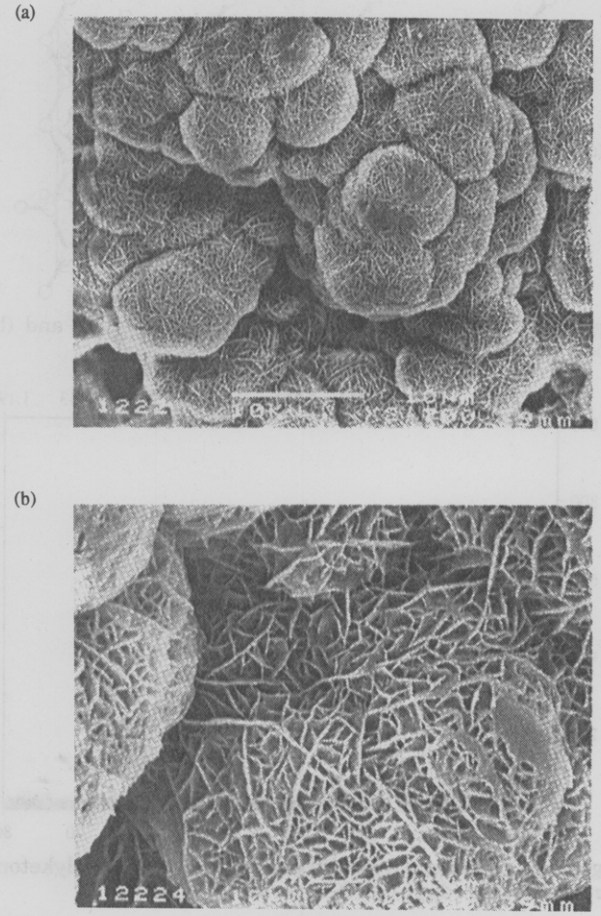

Figure 7. SEI micrograph of a representative sample of polyketones prepared with (dppp)Pd(OAc)$_2$/[(^{t}Bu)AlO]$_6$: (a) ×2700 and (b) ×10000. Figure reduced to 60% for publication.

Figure 8. SEI micrographs of a polyketone film.

However, as is clearly seen from Figure 2 the maximum polymer yield is obtained at *ca.* 75 °C, significantly higher than for the maximum polymer molecular weight. This suggests that while the polymer yield increases to 75 °C, M_n decreases above 50 °C. This result is consistent with the increased occurrence of a chain termination step at higher temperatures, without decreased overall catalytic activity. The polymer molecular weights for polymers prepared under different initial pressures are shown in Figure 11. The average molecular weight of the polyketone increases with increased pressure. This trend is consistent with the rate dependence of polymerization on the initial reaction pressure; i.e., higher pressures result in greater solubility of the reagent gases under the mass transport limit regime and hence an increased polymerization rate.

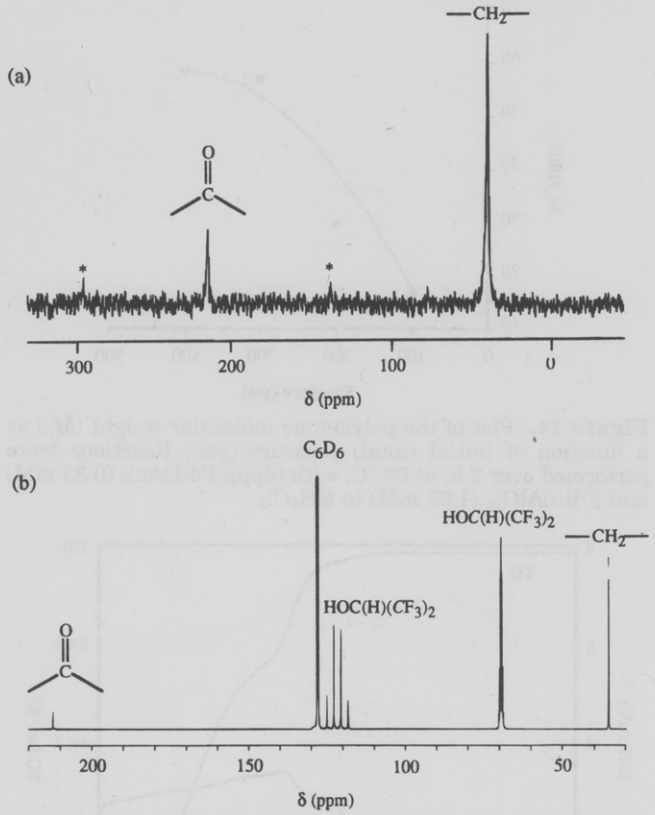

Figure 9. Solid state CPMAS (a) and solution, in HOC(H)-$(CF_3)_2$, (b) ^{13}C NMR spectra of palladium–alumoxane prepared polyketone.

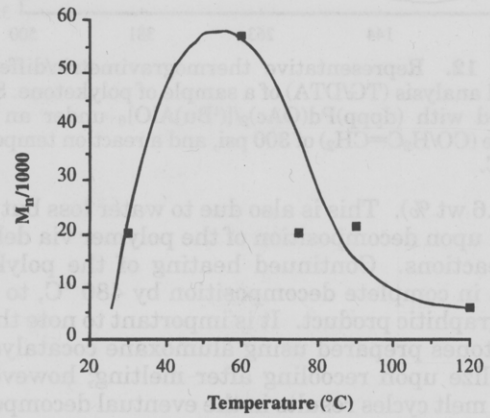

Figure 10. Polyketone molecular weight (M_n) as a function of reaction temperature (°C). Reactions were performed over 2 h, at 300 psi, with (dppp)Pd(OAc)$_2$ (0.33 mM) and [(^{t}Bu)-AlO]$_6$ (1.67 mM) in CH_2Cl_2.

The melting point of high molecular weight polyketones is invariant at 257 °C. Lowering of the melting point has been attributed to the formation of terpolymers (see below) or oligomer (M_n > 1000) rather than polymer (M_n = 20 000–60 000) formation. However, despite the high molecular weights determined for the polyketones produced using the palladium–alumoxane catalyst system, their melting points, as measured by differential thermal analysis (DTA) or differential scanning calorimetry (DSC), are lower than those of polyketone (257 °C) by 20–25 °C; see Table 1.

A typical TG/DTA for the alumoxane cocatalyzed polyketones is shown in Figure 12. As previously reported, polyketones undergo mass loss (0.40–0.97 wt %) above *ca.* 70 °C prior to melting at *ca.* 246 °C. This mass loss has been attributed to the loss of water from the polymer. A second mass loss occurs upon melting

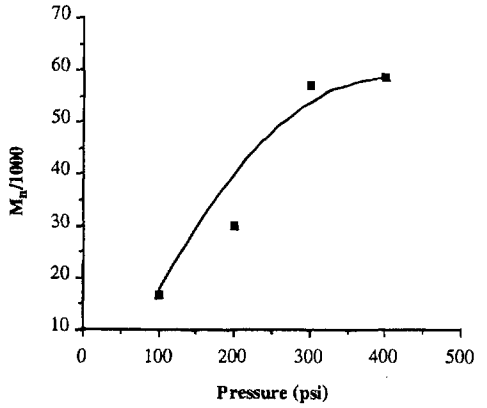

Figure 11. Plot of the polyketone molecular weight (M_n) as a function of initial (total) pressure (psi). Reactions were performed over 2 h, at 60 °C, with (dppp)Pd(OAc)$_2$ (0.33 mM) and [(^{t}Bu)AlO]$_6$ (1.67 mM) in CH_2Cl_2.

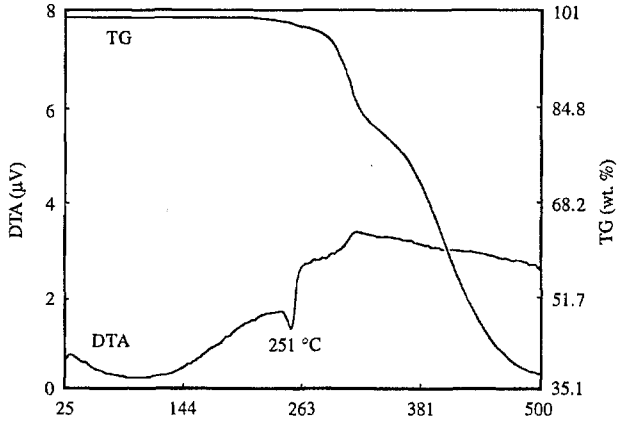

Figure 12. Representative thermogravimetric/differential thermal analysis (TG/DTA) of a sample of polyketone. Sample prepared with (dppp)Pd(OAc)$_2$/[(^{t}Bu)AlO]$_6$ under an initial pressure (CO/H_2C=CH_2) of 300 psi, and a reaction temperature of 60 °C.

(1.6–3.6 wt %). This is also due to water loss but water formed upon decomposition of the polymer via dehydration reactions. Continued heating of the polyketone results in complete decomposition by 480 °C, to give a black graphitic product. It is important to note that the polyketones prepared using alumoxane cocatalysts recrystallize upon recooling after melting; however, repeated melt cycles results in the eventual decomposition of the polymer. It should be noted that unlike polyketones previously, the DTA (see Figure 12) or DSC of the polymers prepared using the alumoxane cocatalyst does not show any evidence for phase transformation above 150 °C.

Polyketone, prepared from carbon monoxide and ethylene has been reported to crystallize in two forms: α- and β-phases. The α-phase has the carbonyl groups in adjacent chains in the structure pointing in about the same direction (approximately along the *b*-axis) at equal heights (along the *c*-axis); see Figure 13a.[27] By contrast, the β-phase has the carbonyl groups of the chains at the corners of the cell pointing in a different direction from those of the chain in the center of the cell; see Figure 13b.[28] Thus, while the polymer chains are the same in each phase, the orientation of the carbonyl groups along the chain is less ordered in the β-phase. A representative powder X-ray diffraction (XRD) of polyketone prepared using (dppp)Pd(OAc)$_2$ and [(^{t}Bu)Al(O)]$_6$ is shown in Figure 14, and is consistent with the α-phase. However, on the basis of peak *d*

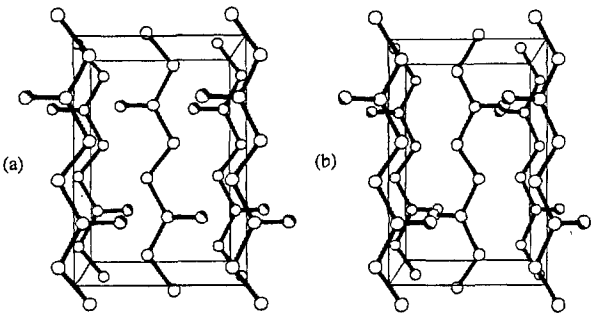

Figure 13. Crystal structures of (a) α-polyketone and (b) β-polyketone, viewed with the fiber axis vertical.

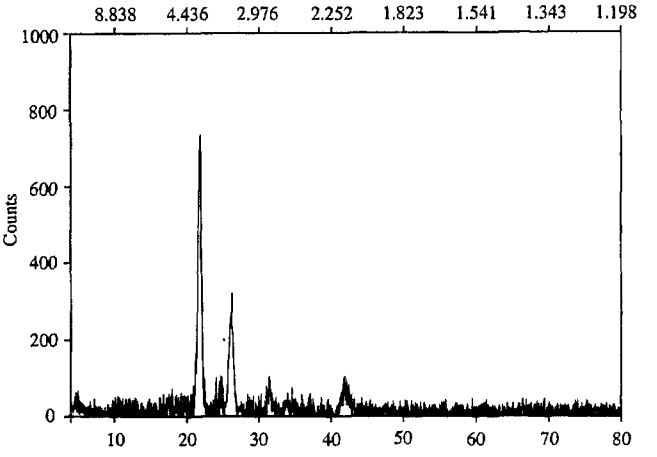

Figure 14. Powder X-ray diffraction of samples of polyketone prepared using (dppp)Pd(OAc)$_2$ with [(^{t}Bu)AlO]$_6$.

Table 2. Crystallographic *d* Spacing of Polyketone Polymers Prepared Using the Palladium/Alumoxane Catalyst[a]

	d spacing (Å)		
hkl	ECO	EOCO	EBPCO
101	4.991	5.010	5.038
110	4.034	4.082	4.077
111	3.557	3.589	3.587
200	3.398	3.456	3.442
112	2.826	2.844	2.835
113	2.136	2.151	2.150

[a] ECO = ethylene/CO, EOCO = ethylene/1-octene/CO, EBPCO = ethylene/4-phenyl-1-butene/CO.

Table 3. Summary of Crystal Unit Cell Parameters and Calculated Crystal Densities for Polyketone Polymers Prepared Using the Palladium/Alumoxane Catalyst

polymer[a]	a	*b* (Å)	*c* (Å)	V (Å^3)	d_{calc} (g·cm^{-3})
ECO[b]	6.79	5.02	7.55	257.3	1.445
	(6.91)	(5.12)	(7.60)	268.8	1.383
EOCO	6.90	5.06	7.59	264.9	1.40–1.50[c]
EPBCO	6.87	5.06	7.59	263.8	1.41–1.53[c]

[a] ECO = ethylene/CO, EOCO = ethylene/1-octene/CO, EPBCO = ethylene/4-phenyl-1-butene/CO. [b] Literature values in parentheses. [c] Density calculated assuming both domains of pure ECO and inclusion of one substituted olefin per ethylene.

spacings the orthorhombic unit cell, space group *Pbnm* (Table 2), for the palladium/alumoxane-prepared polyketone is significantly smaller than observed for polymers prepared with alternative catalysts and than reported in the literature; see Table 3.[27] As can be seen from Table 3, the most significant change observed is in the *a* cell constant, i.e., the direction most associated with interchain packing. The decrease in cell volume is accompanied by a concurrent increase in density; 1.445

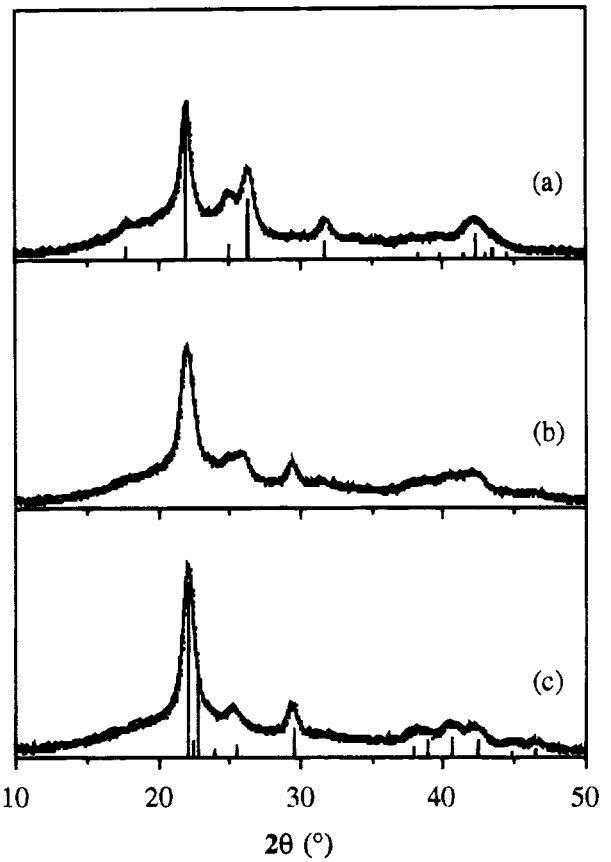

Figure 15. XRD of a sample of polyketone before (a) and after (b, c) thermolysis at 160 °C for 60 h (b) and 100 h (c). The theoretical XRD patterns for α- and β-polyketone are shown for reference.

g·cm^{-3} for the palladium/alumoxane-catalyzed polymer, as opposed to 1.383 g·cm^{-3} as reported in the literature.[27]

The α-phase has been proposed as the low-temperature form, which undergoes a facile phase transition to the β-phase above 150 °C. As noted above, no phase transformation is observed by DTA or DSC measurements, for the polyketones produced using the alumoxane cocatalysts. However, prolonged heating at 160 °C results in the slow conversion of the α-phase to the β-phase; see Figure 15. An alternative reason has been proposed for the observation of different crystallographic phases of polyketones. It has been proposed that the change in crystal structure is due to defects in the chains. The highly ordered α-phase is due to the perfectly alternating ethylene–carbon monoxide copolymer, while the formation of the β-phase is the result of molecular defects in the polymer chain. These defects are possibly due to double insertion of either ethylene, resulting in $-(CH_2)_4-$ units being incorporated, or are a consequence of intrachain furanization. This explanation holds some credence since the NMR spectrum of the β-phase formed upon long term thermolysis does contain resonances consistent with the degradation of the $[-CH_2CH_2C(O)-]_n$ unit. Given that the degradation of polyketones via aldol condensations is catalyzed by the presence of acid residues, and if the β-phase is a consequence of chain defects, then it is reasonable to propose that the facile α- to β-phase transition previously observed is related to the use of acid cocatalysts. We are continuing our investigation of this uncharacteristic phase stability for polyketones formed from ethylene and carbon monoxide.

Synthesis and Characterization of Polyketone Terpolymers. The high melting point of the polyketone derived from ethylene and CO (often referred to as ECO), accompanied as it is with facile catastrophic dehydration, has led to the investigation of terpolymers formed as a result of the inclusion of a primary olefin.[7,14,29–31] The majority of effort has been aimed at terpolymers based on ethylene–propylene–carbon monoxide (EPCO) copolymerization. We have investigated the application of the alumoxane-cocatalyzed system for the new terpolymers: ethylene–(1-octene)–carbon monoxide (EOCO, **IV**) and ethylene–(4-phenyl-1-butene)–carbon monoxide (EPBCO, **V**).

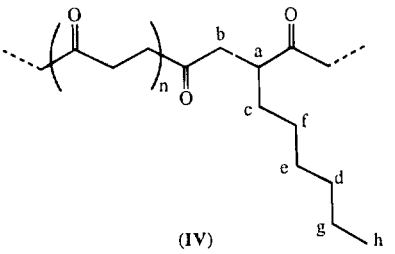

(IV)

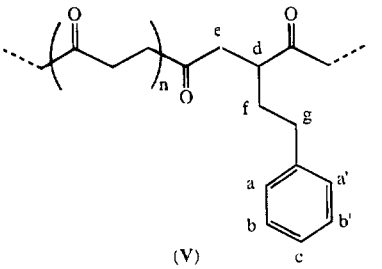

(V)

Addition of an excess of either 1-octene or 4-phenyl-1-butene to the (dppp)Pd(OAc)$_2$/[(^{t}Bu)AlO]$_6$ catalyst solution prior to pressurization with ethylene and CO results in the incorporation of the respective substituted olefin into the parent polyketone chain. The presence of terpolymers is confirmed by IR and NMR spectroscopy, as well as the observation that in the absence of ethylene no polymerization is observed. The IR spectra of the terpolymers show the presence of a broad carbonyl stretch, consistent with the presence of multiple carbonyl units, i.e., $-CH_2CH_2C(O)CH(R)CH_2-$. The terpolymers may also be characterized by NMR spectroscopy. The assignments for the ^{13}C NMR spectra are given in the Experimental Section and are consistent with the insertion of the substituted olefin into the polyketone chain. From the integration of the NMR signal the extent of substitution may be determined; see below.

The terpolymers show significant crystallinity, as evidenced from their XRD; representative examples for EOCO and EPBCO are shown in Figure 16b,c, respectively. On the basis of a comparison of the XRD for the parent polyketone (Figure 16a) it is clear that the terpolymers are of a similar structure, i.e., that of the α-phase orthorhombic, *Pbnm* (see Table 2). However, the calculated unit cell for each of the terpolymers is larger than that of the unsubstituted polyketone, Table 3.[27] The observation that the terpolymers are isostructural with the parent polyketone (ECO) suggests that they are a mixture of crystalline polymer domains consisting of ECO-like material, and amorphous regions in which the large substituents reside. It is interesting to note that the unit cell dimensions, volume, and calculated density of the terpolymers are close to the literature values for polyketone (ECO).[27]

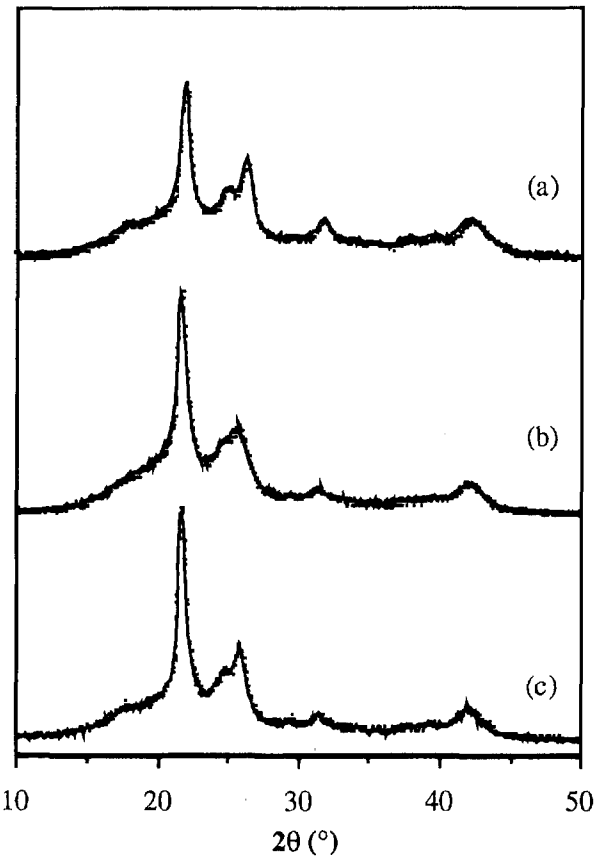

Figure 16. XRD of a sample of polyketone derived from ethylene/CO (a, ECO), ethylene/1-octene/CO (b, EOCO), and ethylene/4-phenyl-1-butene/CO (c, EPBCO).

Table 4. Summary of Catalysis Conditions and Polymer Characterization for Ethylene–(1-Octene)–Carbon Monoxide (EOCO) Terpolymers[a]

sample	temp (°C)	pressure (psi)	yield (mg)[b]	octene:ethylene ratio[c]	T_m (°C)	mass loss (%)
1	45	320	43	1:27	219	6.9
2	60	120	9	0:1	235	6.4
3	60	320	80	1:27	223	13.2
4	60	440	68	1:45	230	15
5	75	320	66	1:24	220	10

[a] All samples were prepared with an excess of 1-octene. [b] Isolated yield. [c] Determined by ^{1}H NMR.

The rate of polymerization of the terpolymers was found to be comparable with that of the parent polyketone. For a typical reaction, using $[(^t\text{Bu})\text{AlO}]_6$ and $(\text{dppp})\text{Pd}(\text{OAc})_2$, and an initial CO/ethylene pressure of 320 psi, the relative yield of parent polyketone and the terpolymers is 317 and 295 mg, respectively. In Table 4 are summarized the reaction conditions and the polymer characteristics for the copolymerization of carbon monoxide, ethylene, and 1-octene (EOCO). As was observed for the parent polyketone synthesis, the polymer yield is dependent on the reaction temperature and the initial pressure. While the ethylene:1-octene ratio is dependent on the pressure of CO/C_2H_4, increased pressure decreases the octene:ethylene ratio, it is independent of the reaction temperature. The maximum value obtained for the incorporation of the substituted olefin represents a 24:1 ethylene:1-octene ratio, even under conditions of large excess. This maximum represents the ratio of the rate constants (k_i) for insertion of $H_2C{=}CH_2$ versus $H_2C{=}C(H)R$ (k_i^a/k_i^b in Scheme 1) and indicates that substitution at the C=C has a

Scheme 1. Insertion of $H_2C{=}CH_2$ versus $H_2C{=}C(H)R$ during the Growth of Terpolymers.[a]

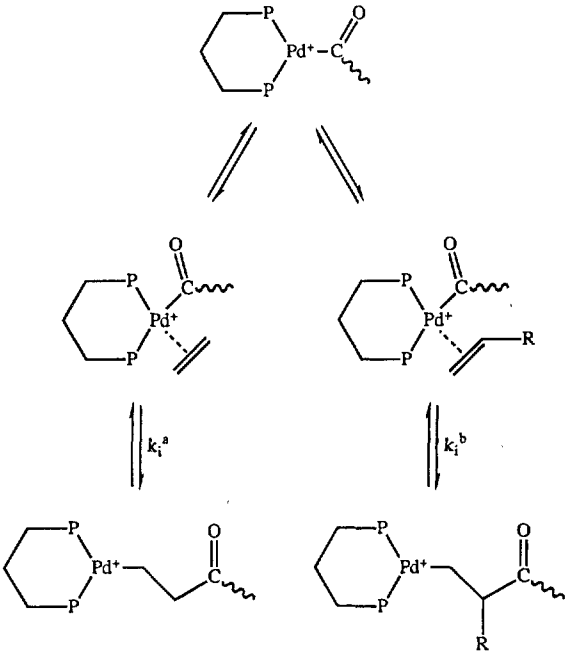

[a] While there is no direct evidence of the regiochemistry of the insertion of the α-olefin, primary insertion is assumed on the basis of steric hindrance arguments.

Table 5. Summary of Molecular Weight Data for Terpolymers with Respect to the Parent Polyketone[a]

polymer[b]	M_w	M_n	R
ECO	122 000	57 100	2.13
EOCO	104 000	62 200	1.68
EPBCO	89 100	55 600	1.60

[a] All samples prepared at 300 psi pressure of ethylene/CO and 60 °C, molecular weights measured in $HOC(H)(CF_3)_2$. [b] ECO = ethylene/CO, EOCO = ethylene/1-octene/CO, EPBCO = ethylene/4-phenyl-1-butene/CO.

significant effect on the rate, i.e., $k_i^a/k_i^b = 24$. The similarity of the rate of insertion of 1-octene and 4-phenyl-1-butene indicates that substitution on the olefin side chain has a minimum effect on olefin insertion.

The as synthesized powder-like terpolymer samples exhibit broad melting endotherms (see Table 4) at temperatures 5–15 deg lower than their ECO counterparts. After a thin film formation as described in the Experimental Section, however, the film sample showed a sharp melting endotherm at a slightly higher temperature. The molecular weights of the terpolymers (see Table 5) are only slightly lower compared to the parent polyketone prepared under identical conditions. However, the polydispersities, R, are significantly lower for the terpolymer.

Conclusions

We have reported that polyketone polymers may be synthesized using a palladium catalyst with an isolable *tert*-butylalumoxane as an alternative cocatalyst to those previously reported. The polymers are perfectly alternating ethylene/CO, are of high molecular weights, and show no spectroscopic evidence for furanization or cross-linking. The crystal structure of the palladium/alumoxane catalyzed polymers is that of the α-phase polyketone. However, the densities of our polyketones are significantly higher than samples of polyketones

prepared using traditional palladium/noncoordinating anion catalyst systems. This increased density is a consequence of a decrease in the interchain packing distances. The palladium/alumoxane-catalyzed polyketones also do not show the facile α- to β-phase transformation observed for polyketones prepared using other catalysts. Extreme conditions (100 h at 160 °C) are required to cause the phase transformation. Terpolymers prepared by the addition of up to 4% of either 1-octene or 4-phenyl-1-butene exhibit crystalline domains with lattice parameters close to those reported previously for the unsubstituted polyketone. Furthermore, the terpolymers appear to undergo the α- to β-phase transformation.

On the basis of the spectroscopic and crystallographic evidence reported herein we propose that the polyketone polymers prepared using the palladium/alumoxane catalyst system are perfectly alternating ethylene carbon monoxide copolymers with no detectable chain defects. The addition of defects (either chain substituents or defects introduced due to thermal decomposition) into the polyketone chain cause an increase in the interchain packing distances, as observed from decreased density. Further polymer degradation results in a phase transformation in which the density increases further. The reasons for the formation of high-density polyketone using the palladium/alumoxane catalyst are at present unclear. We are at present investigating the catalytic system in detail, and these results will be reported elsewhere.

Experimental Section

All synthetic procedures were performed under purified nitrogen using standard Schlenk techniques or in an argon atmospheric VAC glovebox unless otherwise mentioned. Solvents were distilled and degassed prior to use. Carbon monoxide, ethylene, and carbon monoxide/ethylene mixture (48.7% CO) gases were obtained from Matheson Gas.

Infrared spectra (4000−400 cm^{-1}) were obtained using a Nicolet 5ZDX-FTIR spectrometer; samples were prepared as CH_2Cl_2 solutions. Solution NMR spectra were obtained on either a Bruker AM-500 or AM-400 spectrometer using C_6D_6/$HOC(H)(CF_3)_2$. Thermogravimetric analyses were obtained on a Seiko 200 TG/DTA instrument using an argon carrier gas. XRD data were collected on a Scintag diffractometer operating at 45 kV and 35 mA. Diffraction management systems (DMS) software operating on a micro-VAX computer was used to interpret the data. SEM studies were performed on a JEOL JSM-35 scanning microscope. $(dppp)Pd(OAc)_2$ was used as received. (dppp)Pd[C(O)^{t}Bu]Cl was prepared as described elsewhere.[32]

Copolymerization of Carbon Monoxide with Ethylene. Copolymerizations were carried out in an autoclave (Berghof, Germany) equipped with a Teflon liner (105 mL). In a typical reaction run, $[(^t Bu)AlO]_6$ (0.025 mmol) was placed in the autoclave under a N_2 atmosphere. The autoclave was then purged with dry carbon monoxide gas for 5 min. A stock solution (0.33 mM in dichloromethane) of $(dppp)Pd(OAc)_2$ (15 mL) was transferred into the autoclave under carbon monoxide atmosphere using an appropriate syringe. The autoclave was then pressurized with the reactant gases at room temperature. When carbon monoxide and ethylene were applied separately, carbon monoxide was applied first. The autoclave was placed in a heating unit, and the reaction was carried out at 60 °C under vigorous stirring. At the end of a set period of time, heating was discontinued and the autoclave was allowed to cool to ambient temperature for 10 min before it was disassembled. Following filtration, the product was allowed to dry in air to provide a white powder. Where necessary, the product was washed with hexane (10 mL) and subsequently with CH_2Cl_2 (10 mL).

Preparation of the Polyketone Films. A polyketone (100 mg, prepared at 400 psi initial CO/ethylene pressure) was dissolved in $HOC(H)(CF_3)_2$ (2.0 mL). This solution was poured over a flat glass surface and allowed to dry under the atmosphere. The film was peeled apart from the glass to be submitted for further analysis.

Terpolymerization of 1-Octene, Carbon Monoxide, and Ethylene. In a typical reaction run, $[(^t Bu)AlO]_6$ (0.025 mmol) was placed in the autoclave under an Ar atmosphere. A stock solution (0.33 mM in dichloromethane) of $(dppp)Pd(OAc)_2$ (15 mL) was transferred into the autoclave under an Ar atmosphere. The autoclave was then pressurized with the carbon monoxide/ethylene mixture at room temperature. Then neat 1-octene (5 mL, 31.8 mmol) was added using an appropriate syringe. The autoclave was placed in a heating unit, and the reaction was carried out at 60 °C under vigorous stirring. At the end of a set period of time, heating was discontinued and the autoclave was allowed to cool to ambient temperature for 10 min before it was disassembled. Following filtration, the product was rinsed with CH_2Cl_2 (5 mL) and then allowed to dry in air to provide a white powder. ^{13}C NMR [$HOC(H)(CF_3)_2/C_6D_6$, assignment shown in **IV**]: δ 46.8 (*C*H, a), 43.5 (*C*H_2, b), 31.7 (*C*H_2, c), 31.5 (*C*H_2, d), 29.3 (*C*H_2, e), 27.1 (*C*H_2, f), 22.6 (*C*H_2, g), 13.3 (*C*H_3, h).

Terpolymerization of 4-Phenyl-1-butene, Carbon Monoxide, and Ethylene. This compound was prepared using a procedure analogous to that described for 1-octene/carbon monoxide/ethylene terpolymer. 4-Phenyl-1-butene (5 mL, 33.3 mmol) was used in place of 1-octene. ^{13}C NMR [$HOC(H)(CF_3)_2$/$CDCl_3$, assignment shown in **V**]: δ 129.1 (*C*H, a, a′), 129.0 (*C*H, b, b′), 128.9 (*C*H, c), 46.2 (*C*H, d), 43.3 (*C*H_2, e), 33.0 (*C*H_2, f), 32.8 (*C*H_2, g).

Acknowledgment. Financial support of this work was provided by the Office of Naval Research. The assistance of Dr. Patrick Perrot with SEM measurements is gratefully acknowledged. GC−MS measurements were performed with the assistance of Dr. A. Tyler (Harvard University). We are indebted to Dr. Janet Braddock-Wilking (University of Missouri, St. Louis), Dr. A. J. Perrotta and R. B. Minnick (Alcoa Technical Center), and Dr. S. Ittel (DuPont) for assistance with solid state NMR, surface area, and molecular weight measurements, respectively.

References and Notes

(1) (a) Brubaker, M. M.; Coffman, D. D.; Hoehn, H. H. *J. Am. Chem. Soc.* **1952**, *74*, 1509. (b) Brubaker, M. M. U.S. Patent 2 495 286, 1950.
(2) (a) Starkweather, H. W. Olefin-Carbon Monoxide Copolymers; Encyclopedia of Polymer Science and Engineering, 2nd ed.; John Wiley: New York, 1987; Vol. 10. (b) Starkweather, H. W. *J. Polym. Sci. Polym. Phys. Ed.* **1977**, *15*, 247.
(3) For reviews of polyketone synthesis, see: (a) Sen, A. The Copolymerization of Carbon Monoxide with Olefins; Advances in Polymer Science; Springer-Verlag: Berlin, 1986; Vols. 73−74. (b) Sen, A. *CHEMTECH* **1986**, 48.
(4) Shryne, T. M.; Holler, H. V. U.S. Patent 3,984,388, 1976.
(5) (a) Nozaki, K. German Patent 2,414,260, 1974. (b) Nozaki, K. U.S. Patent 3,835,123, 1974.
(6) (a) Nozaki, K. U.S. Patent 3,694,412, 1972. (b) Nozaki, K. U.S. Patent 3,689,460, 1972.
(7) Sen, A.; Lai, T. *J. Am. Chem. Soc.* **1982**, *104*, 3520.
(8) Lai, T.; Sen, A. *Organometallics* **1984**, *3*, 866.
(9) See for example: (a) Drent, E.; Wife, R. L. U.S. Patent 4,970,294, 1990. (b) Van Leeuwen, P. W. N.; Roobeek, C. F.; Wong, P. K. Eur. Pat. Appl. EP 393,790, 1990. (c) Drent, E. Eur. Pat. Appl. EP 390,292, 1990.
(10) See: (a) Brookhart, M.; Grant, B.; Volpe, A. F., Jr. *Organometallics* **1992**, *11*, 3920. (b) Brookhart, M.; Rix, F. C.; DeSimone, J. M. *J. Am. Chem. Soc.* **1992**, *114*, 5894.
(11) Chepaikin, E. G.; Bezruchenko, A. P.; Belov, G. P. *Izv. Akad. Nauk SSSR, Ser. Khim.* **1990**, *9*, 2181.
(12) Drent, E.; Van Broekhoven, J. A. M.; Doyle, M. J. *J. Organomet. Chem.* **1991**, *417*, 235.
(13) Klaubunde, U.; Tulip, T. H.; Roe, D. C.; Ittel, S. D. *J. Organomet. Chem.* **1987**, *334*, 141.

(14) Sen, A.; Jiang, Z. *Macromolecules* **1993**, *26*, 911.
(15) See for example: (a) Sinn, H.; Kaminsky, W. *Adv. Organomet. Chem.* **1980**, *18*, 99. (b) Sinn, H.; Kaminsky, W.; Vollmer, H. J.; Woldt, R. *Angew. Chem., Int. Ed. Engl.* **1980**, *92*, 390. (c) Sishta, C.; Hathorn, R. M.; Marks, T. J. *J. Am. Chem. Soc.* **1992**, *114*, 1112. (d) Jordan, R. F. *Adv. Organomet. Chem.* **1991**, *32*, 325.
(16) Straub, S. H. *Chem. Rev.* **1993**, *93*, 927.
(17) Pasynkiewicz, S. *Polyhedron* **1990**, *9*, 429.
(18) Cooley, N. A. Eur. Patent 590,942, 1994.
(19) Mason, M. R.; Smith, J. M.; Bott, S. G.; Barron, A. R. *J. Am. Chem. Soc.* **1993**, *115*, 4971.
(20) Harlan, C. J.; Mason, M. R.; Barron, A. R. *Organometallics.* **1994**, *13*, 2957.
(21) Harlan, C. J.; Bott, S. G.; Barron, A. R. *J. Am. Chem. Soc.* **1995**, *117*, 6465.
(22) 100 psi = 5170 Torr = 6.89 bar.
(23) Those polymers prepared at temperatures higher than 80 °C possess a gray tinge, possibly due to the presence of finely divided palladium metal.
(24) See for example: (a) Starkweather, H. W., Jr., *J. Polym. Sci., Polym. Phys. Ed.* **1977**, *15*, 247. (b) Wittwer, H.; Pino, P.; Suter, U. W. *Macromolecules* **1988**, *21*, 1262. (c) Hoyer, H.; Fitzky, H. G. *Makromol. Chem.* **1972**, *161*, 49. (d) Conti, G.; Sommazzi, A. *J. Mol. Struct.* **1993**, *294*, 275. (e) Chepaikin, E. G.; Bezruchenko, A. P.; Belov, G. P. Izv. *Akad. Nauk SSSR, Ser. Khim.* **1990**, *9*, 2181.
(25) Koide, Y.; Barron, A. R. *Main Group Met. Chem.* **1995**, *18*, 405.
(26) The polyketone prepared at 120 °C has a low M_n as a consequence of the presence of a significant content of low molecular weight material, $M_w \approx 3000$.
(27) Lommerts, B. J.; Klop, E. A.; Aerts, J. *J. Polym. Sci., Polym Phys.* **1993**, *31*, 1319.
(28) Chatani, Y.; Takizawa, T.; Murahashi, S.; Sakata, Y.; Nishimura, Y. *J. Polym. Sci.* **1961**, *55*, 811.
(29) (a) Xu, F. Y.; Chien, J. C. W. *Macromolecules* **1993**, *26*, 3485. (b) Xu, F. Y.; Zhao, A. X.; Chien, J. C. W. *Makromol. Chem.* **1993**, *194*, 2579.
(30) Buijsingh, P. D.; Lindhout, I. U.S. Patent 5,219,982, 1993.
(31) (a) Drent, E. U.S. Patent 5,210,176, 1993. (b) Drent, E.; Keijsper, J. J. Eur. Pat. Appl. EP 522,635 A1, 1993.
(32) Koide, Y.; Bott, S. G.; Barron, A. R. *Organometallics*, in press.

MA951369P